Effect of Molecular Additives on Electron Mobility and Electron−Ion Recombination Rate Constant in Dense Gaseous Krypton

Mariusz Wojcik*,†,‡,§ and M. Tachiya*,‡,||

Institute of Applied Radiation Chemistry, Technical University of Lodz, Wroblewskiego 15, 93-590 Lodz, Poland, and National Institute of Advanced Industrial Science and Technology (AIST), Tsukuba, Ibaraki 305-8565, Japan

Received: October 22, 2001; In Final Form: January 30, 2002

The rate constant of bulk electron−ion recombination is calculated for dense gaseous krypton doped with CH_4 and N_2. In the calculations, the electron scattering is modeled by experimental, energy-dependent collision cross sections. The applicability of the assumed cross sections is verified by calculations of the electron mobility in Kr/CH_4 and Kr/N_2, which give a reasonable agreement with experiment. For both Kr/CH_4 and Kr/N_2, the recombination rate constant is found to increase with increasing concentration of the molecular species, due to efficient dissipation of electron energy in vibrationally and rotationally inelastic collisions. The simulation results are compared with experimental data, which also demonstrate an enhancement of the recombination rate by molecular additives.

I. Introduction

The bulk electron−ion recombination in dense gaseous argon and krypton has been studied experimentally by the group of Hatano.[1,2] The recombination rate constants in those gases were found to be much lower than the Debye−Smoluchowski value $k_D = 4\pi e\mu/\epsilon$ predicted by the standard diffusion theory of ion recombination.[3,4] Here, e is the electron charge, μ is the electron mobility, and ϵ is the dielectric constant. The observed inapplicability of the diffusion theory is related to high electron mobilities in dense rare gases, and values of the recombination rate constant lower than k_D were also found in other systems, where the mobility of charges exceeds $\sim$100 cm^2 V^{-1} s^{-1}.[5−7] Several theoretical models[8−13] were proposed to describe the electron−ion recombination in a wide class of high-mobility systems. In many cases, however, those general models were not able to achieve good accordance with experiment. The discrepancies are especially large for gaseous argon and krypton.[2] In such a situation, we have concentrated on studying the recombination processes in rare gases and constructed a theoretical model[14] that reflects the specific nature of those systems. In rare gases, electrons undergo only elastic collisions with gas atoms and, due to a very small mass ratio m/M of the electron to the atom, the dissipation of the electron kinetic energy is very inefficient. In ref 14 we modeled the recombination in argon and krypton by simulating individual electron trajectories, and used experimental, energy-dependent cross sections for elastic collisions to describe the electron scattering. Unfortunately, the recombination rate constants calculated using that approach were found to be lower than the experimental data, and further studies are still needed in order to achieve a satisfactory agreement with experiment. Since the model of the electron scattering assumed in our previous calculations[14] seems to be rather realistic, reasons for the observed discrepancy must be sought in other effects, such as the ion concentration effect, the influence of an external electric field applied in the experimental studies, the assumed recombination criterion, or a possible role of molecular impurities in measured gas samples. In this paper, we concentrate on the last of these effects and calculate the recombination rate constants in dense gaseous krypton doped with methane and nitrogen. In the presence of molecular impurities, electrons may effectively interact with the available vibrational and rotational modes, and dissipate energy much more efficiently than in pure gases. This may significantly increase the recombination rate, even at very low impurity concentrations. Another motivation for this study comes from the fact that the electron−ion recombination rate constants have been recently measured[15] for argon and krypton doped with methane and nitrogen. A direct comparison of the theoretical and experimental data should be helpful in understanding the mechanism of the electron−ion recombination in dense rare gases.

In the calculations presented in this paper we basically follow the methodology developed for modeling the electron−ion recombination in pure rare gases and described in detail in ref 14. We start with gathering cross section data for all types of scattering events encountered by electrons in the analyzed systems. In addition to the cross sections for elastic collisions with krypton atoms, we need to construct sets of cross sections describing both the elastic and inelastic electron scattering by methane and nitrogen. The collected cross sections are used in modeling individual electron trajectories in Kr/CH_4 and Kr/N_2 mixtures. Before calculating the recombination rate constants, we determine for both systems the electric field dependence of the electron mobility. This dependence is used to verify the assumed simulation model by comparison with the corresponding experimental data. Finally, we apply the simulation method developed in ref 14 to calculate the recombination rate constants, and compare the results with experiment.

† Institute of Applied Radiation Chemistry.
‡ National Institute of Advanced Industrial Science and Technology (AIST).
§ E-mail: wojcikm@mitr.p.lodz.pl.
|| E-mail: m.tachiya@aist.go.jp.

10.1021/jp013921k CCC: $22.00
Published on Web 04/17/2002

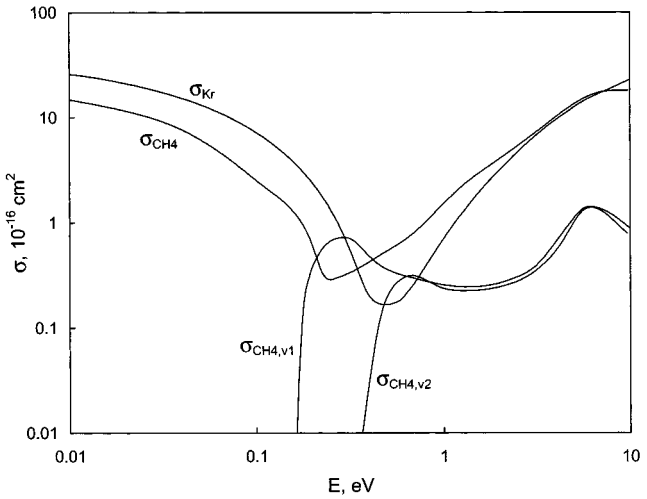

Figure 1. Momentum transfer cross sections for electron collisions with krypton, σ_{Kr}, and methane, σ_{CH_4}, and cross sections for excitation by electron collisions of the two effective vibrational modes of methane, $\sigma_{CH_4,v1}$ and $\sigma_{CH_4,v2}$. Data taken from refs 16 and 18.

II. Calculations for Kr + CH_4

A. Cross Sections. The measurements of the electron−ion recombination rate constant in gaseous krypton,[2] as well as our previous calculations,[14] were carried out for systems of density $\sim 10^{21}$ cm^{-3}. At such high densities, the effects due to the dimer formation or electron multiple scattering are no longer negligible, and the electron transport processes cannot be precisely described by low-pressure scattering data. However, since accurate cross sections for high-density krypton are not available, we decided to use a low-pressure cross section to describe the elastic *e*-Kr collisions. We apply the well-established momentum transfer cross section of Hunter, Carter, and Christophorou[16] as given in their Table 4. The validity of this approach to modeling the electron transport processes in dense gaseous Kr was widely discussed in ref 14. We found that the use of the low-pressure momentum transfer cross section to describe electron scatterings in krypton at gas density as high as $n = 1.2 \times 10^{21}$ cm^{-3} may be regarded as a reasonable approximation.

For methane and for the electron energy range from zero to several eV, the collision processes that should be taken into account are the elastic collisions and two vibrationally inelastic processes.[17,18] The rotational excitation of the highly symmetric methane molecule is expected to be small. For both elastic and vibrationally inelastic *e*-CH_4 collisions, we use the cross sections of Hayashi taken from Figure 1 in ref 18. Those cross sections, together with the momentum transfer cross section for krypton, are plotted in Figure 1. The deep minima in the momentum transfer cross sections for both krypton and methane are due to the Ramsauer−Townsend effect.

The two vibrational cross sections shown in Figure 1, $\sigma_{CH_4,v1}$ and $\sigma_{CH_4,v2}$, describe collisional transitions from the ground state to the first excited states in the two effective vibrational modes of CH_4 (usually denoted by υ_{24} and υ_{13}, respectively[17]). Although methane has four distinguishable vibrational modes, they can be practically reduced to two because of closely lying threshold energies. Following ref 18 we assume the threshold energies for the two effective modes as $E_{CH_4,v1} = 0.162$ eV and $E_{CH_4,v2} = 0.361$ eV. At the temperature chosen in this study, $T = 291$ K, it is reasonable to assume that populations of vibrationally excited states higher than the first excited state in each mode are negligible.

In addition to elastic collisions and inelastic excitations of the vibrational modes of CH_4, we also need to include in our simulations collisional deexcitations of the excited vibrational states. The cross sections for these "superelastic" processes can be obtained from the corresponding excitation cross sections using the principle of microscopic reversibility.[17] In general, this principle relates the cross section for a transition from state j to i, σ_{ji}, with the corresponding cross section for a transition from i to j, σ_{ij}, by

$$\sigma_{ji}(E) = \frac{g_i}{g_j}\frac{E + E_{ij}}{E}\sigma_{ij}(E + E_{ij}) \quad (1)$$

Here, E is the electron energy, E_{ij} is the transition energy from i to j, and g_i and g_j are the degeneracies of the states i and j, respectively. We use eq 1 to calculate deexcitation cross sections for all inelastic processes considered in this study.

B. Electron Mobility. In the calculations of the mobility, we simulate individual electron trajectories in an applied electric field. We start an electron from the origin and select the time to a collision, t_s. Then, we calculate the classical electron trajectory in the constant electric field up to t_s. At that time, we decide the type of collision to take place, and calculate a change of the electron velocity resulting from this collision. Now, we select the next value for t_s, and repeat the procedure many times until a predefined, very long time t_f elapses. By dividing the final electron displacement in the direction of the field by t_f we obtain the electron drift velocity and, hence, the mobility. We carry out the calculations for a number of independently generated electrons, which allows us also to obtain an estimate for the statistical error of the simulation.

For an electron in a Kr/CH_4 mixture we consider the following types of collisions: elastic collisions with krypton atoms (σ_{Kr}) and methane molecules (σ_{CH_4}), collisional excitations of the two effective vibrational modes of methane ($\sigma_{CH_4,v1}$ and $\sigma_{CH_4,v2}$), and collisional deexcitations of the excited vibrational modes ($\sigma_{CH_4,s1}$ and $\sigma_{CH_4,s2}$). The symbols in parentheses denote the corresponding collision cross sections. To effectively model the electron scattering in a system where the collision cross sections depend on velocity, we use the null-collision method.[19−21] In this method, in addition to real electron collisions, we introduce fictitious null collisions, in which the electron velocity, ν, remains unaffected. The cross section $\sigma_n(\nu)$ for the null collisions is chosen in such a way that the total collision rate K_{max} is independent of velocity

$$n_{Kr}\nu\sigma_{Kr}(\nu) + n_{CH_4}\nu\sigma_{CH_4}(\nu) + n_{CH_4}n_{v,0}\nu\sigma_{CH_4,v1}(\nu) + n_{CH_4}n_{v,0}\nu\sigma_{CH_4,v2}(\nu) + n_{CH_4}n_{v,1}\nu\sigma_{CH_4,s1}(\nu) + n_{CH_4}n_{v,2}\nu\sigma_{CH_4,s2}(\nu) + \nu\sigma_n(\nu) = K_{max} = \text{constant} \quad (2)$$

Here, n_{Kr} and n_{CH_4} denote the relative concentrations of krypton and methane ($n_{Kr} + n_{CH_4} = 1$), $n_{v,0}$ is the population of the vibrational ground state of CH_4, $n_{v,1}$ and $n_{v,2}$ are the populations of the first excited states in the two vibrational modes of CH_4, respectively. We assume $n_{v,0} + n_{v,1} + n_{v,2} = 1$. Using the null-collision method, the times between the collisions can be generated from the exponential distribution with the mean value

$$\tau = \frac{1}{nK_{max}} \quad (3)$$

where n is the density. The value of K_{max} is chosen dynamically so that it is bigger than $\nu\sigma_{tot}(\nu)$ on the whole electron trajectory

between the collisions, where $\sigma_{tot}(\nu)$ denotes the total cross section for all types of real collisions. When a collision occurs, it must be decided whether it is a real or a null collision, and, in the former case, which type of a real collision it is. The decision is made at random, with the probability of each event determined by its relative contribution to the total collision rate K_{max}, as described by eq 2.

To model a particular type of a real collision of an electron with velocity **v**, the following simulation procedure is applied. First, we select the velocity of either a krypton atom, $\mathbf{v}_{Kr}$, or a methane molecule, $\mathbf{v}_{CH_4}$, depending on which of these particles participates in the collision, from the Maxwell−Boltzmann distribution. Then, we calculate the new electron velocity from

$$\mathbf{v}' = \frac{m\mathbf{v} + M\mathbf{v}_M}{m+M} + \frac{M}{m+M}\sqrt{u^2 + 2\frac{m+M}{mM}\Delta E}\,\mathbf{n} \quad (4)$$

where m is the electron mass, M is either the atomic mass of Kr or molecular mass of CH_4, depending on the type of collision, and $\mathbf{v}_M$ is either $\mathbf{v}_{Kr}$ or $\mathbf{v}_{CH_4}$, respectively. u is the relative electron velocity before the collision ($\mathbf{u} = \mathbf{v} - \mathbf{v}_M$), and **n** is a random vector of unit length. We assume here that the electron scattering is isotropic in the center of mass system. The energy change ΔE is zero for elastic collisions. For vibrational collisions, $|\Delta E|$ is equal to the threshold energy of a particular vibrational mode participating in the collision, and ΔE is taken negative for vibrational excitations and positive for vibrational deexcitations. Further details of the simulation method used in the calculations of the electron mobility, as well as a discussion of simulation errors, can be found in ref 14.

The simulation results on the electric field dependence of the density-normalized electron mobility in dense gaseous Kr/CH_4 mixtures are shown in the lower part of Figure 2. The calculations were performed for systems of density $n = 1.2 \times 10^{21}$ cm^{-3} and temperature $T = 291$ K. We assumed the dielectric constant of 1.04.[2] Open circles show the results obtained for the methane concentration $c_{CH_4} = 0.05$ mol %, and squares correspond to those obtained for $c_{CH_4} = 0.1$ mol %. Closed circles represent the results for pure krypton calculated in our previous study.[14] The upper part of Figure 2 shows the experimental results for the electron mobility in Kr/CH_4 mixtures obtained by Takeda et al.[15] The three curves show the data obtained for methane concentrations corresponding to those assumed in our calculations, and the meaning of the symbols is the same as in the lower part of the figure. The experiments of Takeda et al. were carried out for $n = 1.7 \times 10^{21}$ cm^{-3} and $T = 290$ K. A comparison between the theoretical and experimental results presented in Figure 2 shows that the simulation method developed in this study is able to reproduce the basic features of the electric field dependence of electron mobility in dense gaseous Kr and Kr/CH_4 mixtures at the methane concentrations considered. For pure krypton, the position of the maximum in the mobility curve, due to the presence of the Ramsauer−Townsend minimum in the scattering cross section, almost exactly matches the corresponding experimental value. The maximum shifts toward higher electric fields with increasing methane concentration. For both $c_{CH_4} = 0.05$ and 0.1 mol %, the calculated values of the mobility at maximum relative to the maximum value in pure Kr are about the same as those observed in experiment. There is, however, a disagreement in the absolute values of the mobility, and the theoretical results are lower by about 25% than the corresponding experimental data. In addition, the peak widths in the calculated mobility curves are wider than those observed in experiment, and the shift of the peak position toward higher fields with increasing methane concentration is faster in the case of the simulation results.

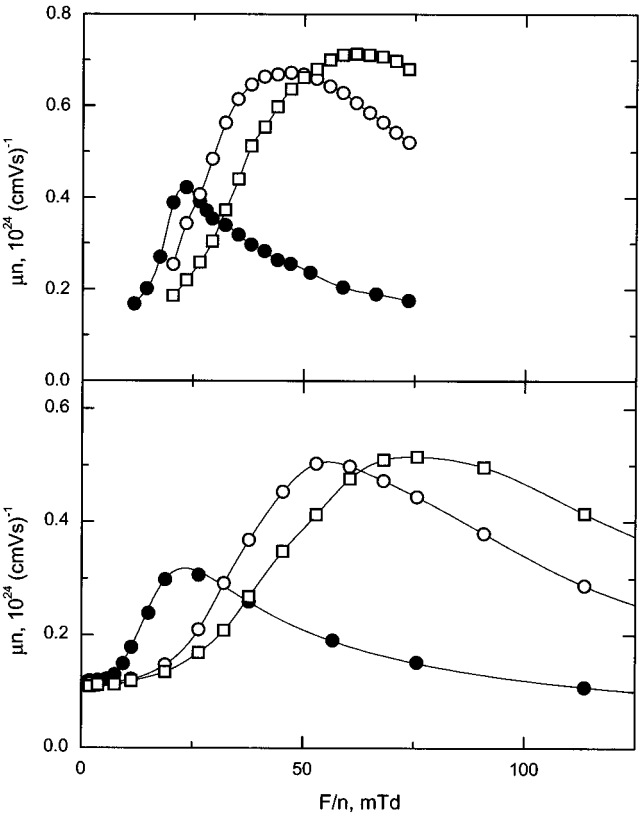

Figure 2. Comparison of the theoretical (lower part) and experimental[15] (upper part) results on the electric field dependence of the density normalized electron mobility in Kr/CH_4. Results for pure Kr (closed circles), and for methane concentrations of 0.05 mol % (open circles) and 0.1 mol % (squares) are presented. 1 mTd = 10^{-20} Vcm^2

The main approximation made in constructing the simulation model of electron scattering applied in this study is the use of the low-pressure cross sections to describe electron collisions in dense gases. The simulation results of the electron mobility in Kr/CH_4 systems are in a reasonable agreement with experiment. Therefore we can consider that at gas densities considered here the above approximation does not have a significant effect on the calculations. In view of this, it seems to be justified to use the proposed simulation model also in the calculations of the electron−ion recombination rate constant.

C. Recombination Rate Constant. The simulation method that we use to calculate the recombination rate constant is based on the method proposed by Northrup et al.[22] We model a system composed of an electron and a cation, and assume that at distances from the cation larger than b the motion of electrons may be described by the Smoluchowski equation. At distances shorter than b, individual trajectories of electrons are simulated and the probability $p(b,E_{crit},q)$ that they recombine rather than separate to a distance q, which is larger than b, is determined. The recombination is assumed to take place when the total relative energy of the electron-cation pair falls below a critical energy E_{crit}.[10,23] The electron trajectories are calculated as classical trajectories in the Coulomb field of the cation. Electrons undergo collisions with either Kr atoms or CH_4 molecules, and both the types of collisions considered and the algorithm used to model those collisions are the same as in the calculations of the electron mobility described in section IIB. The recombination

rate constant k is related to the recombination probability $p(b,E_{crit},q)$ by[14,22]

$$k = \frac{k_D p(b,E_{crit},q)}{\exp\left(-\frac{r_c}{q}\right) - \exp\left(-\frac{r_c}{b}\right)} \quad (5)$$

where r_c is the Onsager radius defined by $r_c = e^2/\epsilon k_B T$, and k_B is the Boltzmann constant.

Since the Kr/CH_4 systems modeled in this study are composed mostly of Kr gas, and the mechanism of dissipating the electron energy in rare gases is very inefficient, the recombination probability to be determined from the simulation is extremely low ($\sim 10^{-6}$). Such a low recombination probability makes its evaluation by simulation infeasible. To overcome this problem we divide the recombination process into two phases, separated in the energy space by a conveniently chosen level E_1. The recombination probability is then calculated as a product of two larger quantities describing the probability of the electron's arriving at E_1 from a higher energy, $p(b,E_1,q)$, and that of arriving at E_{crit} from E_1, $p_{II}(E_1,E_{crit},q)$. The recombination rate constant can now be expressed as[14]

$$\frac{k}{k_D} = \frac{p(b,E_1,q)}{\exp\left(-\frac{r_c}{q}\right) - \exp\left(-\frac{r_c}{b}\right)} p_{II}(E_1,E_{crit},q) = k_I(b,E_1,q) p_{II}(E_1,E_{crit},q) \quad (6)$$

and the quantity $k_I(b,E_1,q)$ may be regarded as a virtual recombination rate constant obtained from the results of phase I of the simulation. Further details of the simulation method used in calculations of the recombination rate constant can be found in ref 14.

In the calculations we use reduced units. We assume r_c as the unit of length, k_BT as the unit of energy, and $(k_BT/m)^{1/2}$ as the unit of velocity. The unit of time is $r_c/(k_BT/m)^{1/2}$.

In phase I of the simulation we start electrons at a distance b from the cation, and follow their motion until either they reach the energy level E_1, or separate to a distance q from the cation ($q > b$). The value of b must be chosen large enough to make the determined quantity k_I independent of that parameter. The dependence of $k_I(b)$ on b for pure krypton was calculated in ref 14. It was found that the asymptotic region of k_I can be reached only for b higher than $100r_c$ [cf. Figure 4b in ref 14]. In those calculations we assumed $E_1 = -0.1k_BT$, and obtained $k_I = 0.138$, with the standard error estimated as 0.018. The calculations in phase I of the simulation for Kr/CH_4 mixtures were performed for methane concentrations of 0.1 and 1 mol %. In both cases we found that in the range of b between $20r_c$ and $40r_c$ the probabilities $p(b,E_1,q)$ are identical, within statistical error, with those obtained for pure krypton in ref 14. Therefore, we decided to skip time-consuming calculations of $p(b,E_1,q)$ for larger values of b, and assumed that the value of k_I determined for Kr can also be used in the calculations of the recombination rate constant in the considered Kr/CH_4 mixtures. This assumption can be justified by the fact that the threshold energies for the vibrational excitations of CH_4 are much higher than the average kinetic energy of electrons in phase I of the simulation. The probability of inelastic collisions in this phase should then be very low. In addition, the contribution of elastic e-CH_4 collisions (σ_{CH_4} is slightly different from σ_{Kr}, cf. Figure 1) to electron scattering should not significantly affect the recombination probability at methane concentrations up to 1 mol %.

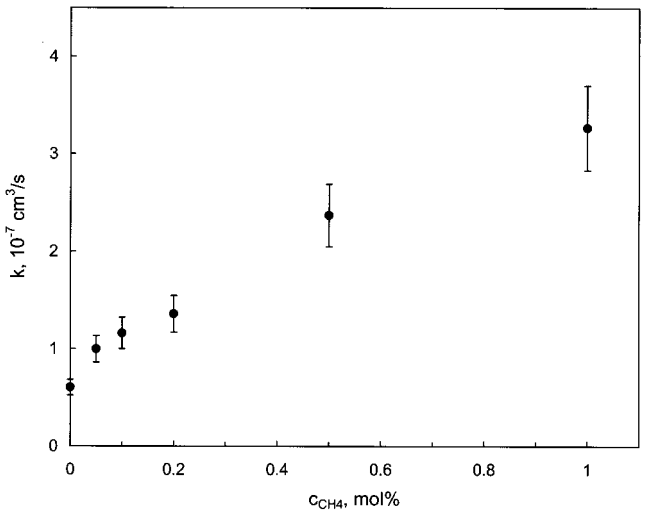

Figure 3. Dependence of the electron−ion recombination rate constant in dense gaseous Kr/CH_4 mixtures on the concentration of methane. The error bars show the standard error of the simulation results.

In phase II of the simulation, we calculate the probability $p_{II}(E_1,E_{crit},q)$ that an electron, started with the total energy E_1, will recombine at the critical energy E_{crit}, rather than escape to a distance q from the cation. As input values for the electron position and velocity we take the values recorded for electrons arriving at E_1 in phase I of the simulation for pure Kr (for $b = 100r_c$). We assume $E_{crit} = -10k_BT$ and $q = 40r_c$. This choice of parameters has been widely discussed in ref 14. The probability p_{II} multiplied by the value k_I determined from phase I of the simulation gives the recombination rate constant relative to k_D [cf. eq 6].

In Figure 3 we present the absolute values of the rate constant k calculated for Kr/CH_4 mixtures at methane concentrations ranging from 0 to 1 mol%. We assume $k_D = 1.67 \times 10^{-4}$ cm^3/s calculated using the value of the zero field electron mobility in krypton $\mu = 95.93$ cm^2 V^{-1} s^{-1} determined in ref 14. From Figure 2 we know that the zero field electron mobility is not affected by the presence of a small concentration of methane. Figure 3 shows that the electron−ion recombination rate constant increases with the concentration of methane added to the gaseous krypton. The rate constant at 0.05 and 0.1 mol % CH_4 is by 65% and 92%, respectively, higher than its value for pure Kr. At $c_{CH_4} = 1$ mol % the increase of more than 5 times is observed. The reasons for such a behavior of k will be discussed in section IV.

III. Calculations for Kr + N_2

A. Cross Sections. In the presence of molecular nitrogen, the electron scattering processes that should be included in the simulation are the elastic collisions with N_2 molecules, and both vibrationally and rotationally inelastic e-N_2 processes. A critical survey of the available cross sections for electron-nitrogen collisions was made by Itikawa et al.[24] We construct the momentum transfer cross section for e-N_2 collisions, σ_{N_2}, from the data presented in Figure 10.1 of ref 24, supplemented with the momentum transfer cross section data provided by Phelps[25] for energies lower than 0.01 eV.

The vibrational ($0 \rightarrow 1$) excitation of the nitrogen molecule has the threshold energy $E_{N_2,v} = 0.289$ eV.[24] The cross section that we use to model this process, $\sigma_{N_2,v}$, is taken from Figures 6.1 and 10.1 of ref 24. We also take into account the collisional ($1 \rightarrow 0$) deexcitation of the vibrational mode of N_2, with the cross section, $\sigma_{N_2,s}$, calculated from $\sigma_{N_2,v}$ using eq 1.

The energies of the rotational levels of N_2 are given by $E_J = BJ(J+1)$, and the rotational constant is $B = 2.467 \times 10^{-4}$ eV.[24] In the simulation, we include collisional processes involving rotational states up to $J_{max} = 30$. Since N_2 molecule has no dipole moment, only quadrupole rotational transitions ($J \rightarrow J \pm 2i$) are allowed. To construct the cross section for the rotational $0 \rightarrow 2$ excitation, σ_{02}, for $E \geq 0.03$ eV we use the cross section calculated by Onda[26] and shown in Figure 10.1 of ref 24, and for $E < 0.03$ eV the cross section obtained from the Gerjuoy−Stein formula[27] is used.

$$[\sigma_{J,J+2}(E)]_{GS} = \frac{8\pi}{15} Q^2 a_0^{\,2} \frac{(J+1)(J+2)}{(2J+1)(2J+3)} \left[1 - \frac{(4J+6)B}{E}\right]^{1/2} \quad (7)$$

Here, Q is the quadrupole moment of N_2 expressed in ea_0^2 units, and a_0 is the Bohr radius. Following ref 24 we take $Q = 1.13$. The cross sections for excitations of higher rotational states of N_2 are calculated from σ_{02} using

$$\sigma_{J,J+2}(E) = \frac{[\sigma_{J,J+2}(E)]_{GS}}{[\sigma_{02}(E)]_{GS}} \sigma_{02}(E) = \frac{3}{2} \frac{(J+1)(J+2)}{(2J+1)(2J+3)} \left[\frac{E-(4J+6)B}{E-6B}\right]^{1/2} \sigma_{02}(E) \quad (8)$$

and the cross sections for rotational deexcitations, $\sigma_{J+2,J}$, are obtained from the corresponding $\sigma_{J,J+2}$ using eq 1. We neglect rotational transitions with $|\Delta J| > 2$, although some authors[24] claim that such transitions may have significant cross sections in the resonance region. The momentum transfer cross section, σ_{N2}, and the cross sections for vibrational, $\sigma_{N_2,v}$, and rotational, σ_{02}, excitations used in our calculations are plotted in Figure 4.

B. Electron Mobility. The simulation method for calculating the electron mobility in a gaseous mixture of krypton and a molecular species has been already described in Sec. IIB. In the calculations for the Kr/N_2 system, we take into account the following electron scattering processes: elastic collisions with krypton atoms and nitrogen molecules, collisional excitation and deexcitation of the vibrational mode of N_2, and nonelastic collisions involving rotational excitation and deexcitation of N_2. We use the null collision method, and the expression for the total collision rate in Kr/N_2 is written as

$$n_{Kr}\nu\sigma_{Kr}(\nu) + n_{N_2}\nu\sigma_{N_2}(\nu) + n_{N_2}n_{v,0}\nu\sigma_{N_2,v}(\nu) + n_{N_2}n_{v,1}\nu\sigma_{N_2,s}(\nu) + \sum_{J=0}^{J_{max}-2} n_{N_2}n_J\nu\sigma_{J,J+2}(\nu) + \sum_{J=2}^{J_{max}} n_{N_2}n_J\nu\sigma_{J,J-2}(\nu) + \nu\sigma_n(\nu) = K_{max} = \text{constant} \quad (9)$$

where n_{Kr} and n_{N_2} are the relative concentrations of krypton and nitrogen ($n_{Kr} + n_{N_2} = 1$); $n_{v,0}$ and $n_{v,1}$ are the populations of the vibrational ground state and the first excited state of N_2, respectively ($n_{v,0} + n_{v,1} = 1$); and n_J are the populations of the rotational states of N_2 ($\sum_{J=0}^{J_{max}} n_J = 1$). When a collision occurs, the decision regarding the type of collision to take place is made at random, with the probability of each event determined by its relative contribution to the total collision rate K_{max}. The simulation procedure for modeling a particular type of collision is the same as that described in section IIB. For rotational $J \rightarrow J+2$ excitations, the energy change is calculated as $\Delta E = -(4J+6)B$, and for rotational $J \rightarrow J-2$ deexcitations, $\Delta E = (4J-2)B$.

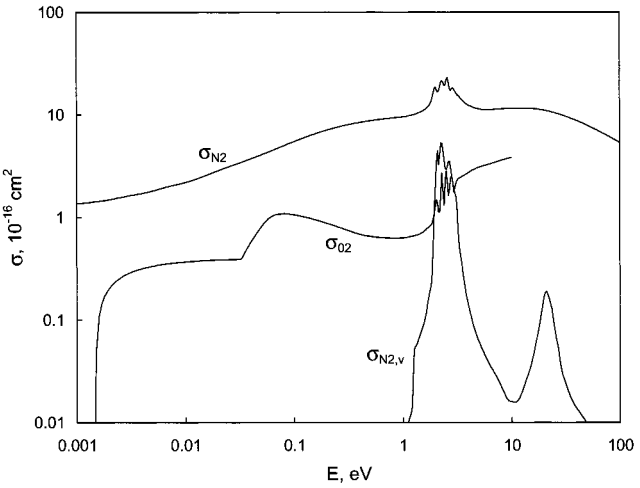

Figure 4. Electron scattering cross sections (c.s.) in N_2: σ_{N_2}, momentum transfer c.s.; $\sigma_{N_2,v}$, c.s. for vibrational ($0 \rightarrow 1$) excitation of N_2; σ_{02}, c.s. for rotational ($0 \rightarrow 2$) excitation of N_2. Data taken from ref 24.

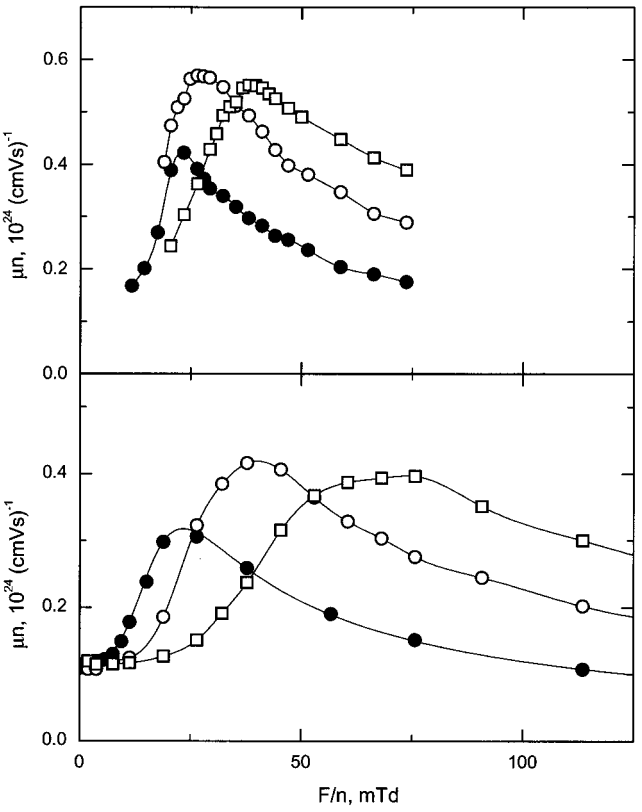

Figure 5. Comparison of the theoretical (lower part) and experimental[15] (upper part) results on the electric field dependence of the density normalized electron mobility in Kr/N_2. Results for pure Kr (closed circles), and for the nitrogen concentrations of 0.5 mol % (open circles) and 2 mol % (squares) are presented.

The calculations of the electron mobility in Kr/N_2 mixtures were performed for the nitrogen concentrations $c_{N_2} = 0.5$ and 2 mol %. The assumed density is $n = 1.2 \times 10^{21}$ cm^{-3} and temperature $T = 291$ K. The simulation results are shown in the lower part of Figure 5, together with the results obtained for pure Kr in our previous study.[14] The upper part of Figure 5 shows the experimental results for the electron mobility in Kr/N_2 mixtures obtained by Takeda et al.[15] In both parts of the figure, the results for pure Kr are shown by closed circles, those for $c_{N_2} = 0.5$ mol % by open circles, and for $c_{N_2} = 2$ mol % by

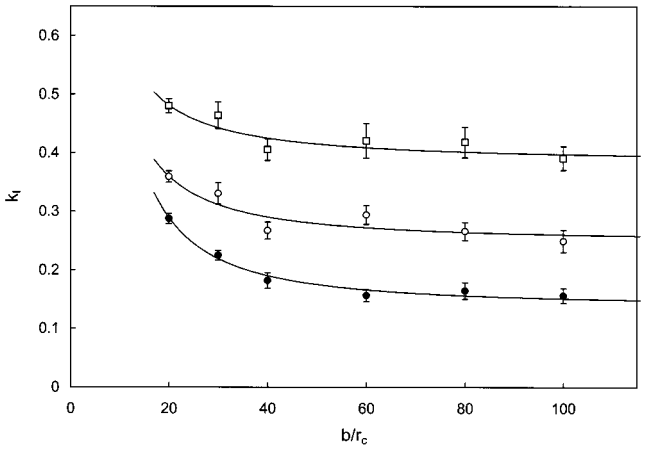

Figure 6. Dependence of the rate constant k_I [defined in eq 6] on the parameter b calculated in phase I of the simulation for Kr/N_2. Results for pure Kr (closed circles), and for the nitrogen concentrations of 2 mol % (open circles) and 5 mol % (squares) are presented. The error bars correspond to the standard error of the simulation results. The solid lines show the regression fits of the results by $k_I(b) = a_1 + a_2 b^{-a_3}$.

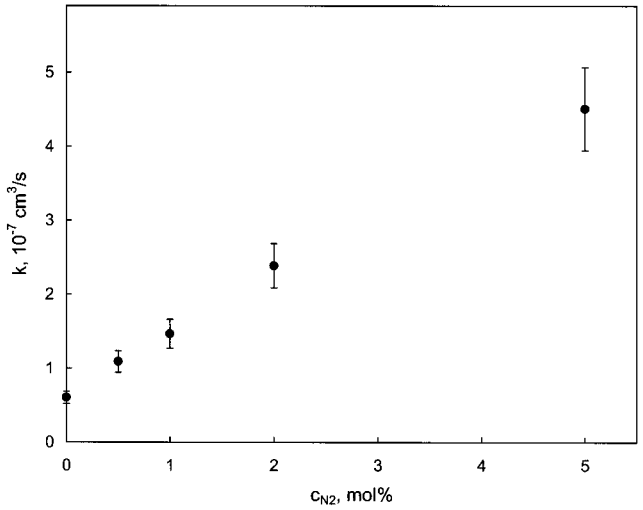

Figure 7. Dependence of the electron−ion recombination rate constant in dense gaseous Kr/N_2 mixtures on the concentration of N_2. The error bars show the standard error of the simulation results.

squares. A comparison between the theoretical and experimental results for Kr/N_2 mixtures leads to conclusions very similar to those in the case of Kr/CH_4. The basic features of the electric field dependence of the density-normalized mobility are correctly reproduced. The maximum in the mobility curve shifts toward higher electric fields with increasing nitrogen concentration. The peak value of the mobility calculated for $c_{N_2} = 0.5$ mol % is by 31% higher than the peak value for pure Kr, while in experiment an increase of 35% is observed. For $c_{N_2} = 2$ mol %, the corresponding numbers are 25% and 30%, respectively. The peak widths in the calculated mobility curves, however, are wider than those observed in experiment, and shift faster toward the higher fields with increasing nitrogen concentration. The absolute values of the calculated mobility are by 25−30% lower than the corresponding experimental data. In conclusion, the simulation results are in a reasonable agreement with experiment, which justifies the use of the constructed simulation model in the calculations of the recombination rate constant.

C. Recombination Rate Constant. In the calculations of the electron−ion recombination rate constant in Kr/N_2 systems we use the same methodology as that applied for Kr/CH_4 and described in section IIC. In the presence of nitrogen, however, we can no longer expect that results of phase I of the simulation will be identical with those obtained for pure Kr. This is due to the fact that electrons may participate in rotationally inelastic e-N_2 collisions even at low kinetic energies they have in phase I of recombination. The significant role of rotationally inelastic collisions in Kr/N_2 is confirmed by the simulation results presented in Figure 6. The figure shows the dependence of the rate constant k_I defined in eq 6 on the value of b, as obtained from the calculations for $c_{N_2} = 2$ mol % (open circles) and 5 mol % (squares). Closed circles show the corresponding results obtained for pure Kr in ref 14. In the calculations, we assumed $E_1 = -0.1k_BT$ and $q = 2b$ in the region $b \leq 60r_c$, outside which $q = b + 40r_c$ was taken. The purpose of this part of calculations was to determine the asymptotic value of k_I at $b \rightarrow \infty$, as a function of c_{N_2}. This was done by fitting an equation $k_I(b) = a_1 + a_2 b^{-a_3}$ to the simulation data, and taking $k_I(b \rightarrow \infty) = a_1$. The calculated asymptotic values of k_I for $c_{N_2} = 0$, 2, and 5 mol % are 0.138, 0.249, and 0.385, respectively, with the standard error estimated as 0.018, 0.030, and 0.046, respectively. The dependence $k_I(c_{N_2})$ is almost linear in the considered range of c_{N_2}.

In phase II of the simulation for Kr/N_2, we determined the recombination probability, $p_{II}(E_1, E_{crit}, q)$, for the nitrogen concentrations ranging from 0.5 to 5 mol %. We assumed $E_{crit} = -10k_BT$ and $q = 40r_c$. In this phase of calculations, as input values for the electron position and velocity we should use the values recorded for electrons arriving at E_1 in the corresponding runs of phase I of the simulation. In the calculations for $c_{N_2} = 2$ and 5 mol %, we read those values from the files obtained for the corresponding nitrogen concentrations and the maximum value of b ($b = 100r_c$). At $c_{N_2} < 2$ mol %, we used the files recorded in phase I of the simulation for pure Kr (for $b = 100r_c$). From separate calculations we know that for c_{N_2} up to 2 mol % the choice of the input file has no significant effect on the results of phase II of the simulation.

In Figure 7 we show the calculated recombination rate constant k in Kr/N_2 mixtures, as a function of the nitrogen concentration. The presented values were obtained by multiplying k_I and p_{II}, determined from the corresponding runs of phase I and phase II of the simulation, respectively, and then by multiplying the results by the Debye−Smoluchowski value k_D [cf. eq 6]. The values of k_I for $c_{N_2} = 0.5$ and 1 mol % were obtained by linear interpolation between the simulation results for pure Kr and for $c_{N_2} = 2$ mol %. From Figure 7 we see that the recombination rate constant increases with the concentration of nitrogen added to krypton. The calculated values of k for $c_{N_2} = 0.5$, 1, 2, and 5 mol % are 1.8, 2.4, 4.0, and 7.5 times higher, respectively, than its value for pure Kr.

IV. Discussion

The purpose of this work was to calculate the effect of addition of a molecular species to a rare gas on the rate constant of bulk electron−ion recombination in that system. We proposed a theoretical approach, in which the electron transport processes are modeled by a direct simulation of both the electron trajectories and electron collisions with atoms and molecules. In rare gases, electrons undergo only elastic collisions. In the presence of a molecular additive, inelastic processes also contribute to electron scattering. We studied both the Kr/CH_4 system, where the collisional interaction with vibrational modes of methane is possible, and the Kr/N_2 system, where rotationally inelastic collisions are also important. To describe all types of collisions, we used the available cross section data. Although we used the cross sections determined for low-pressure gases

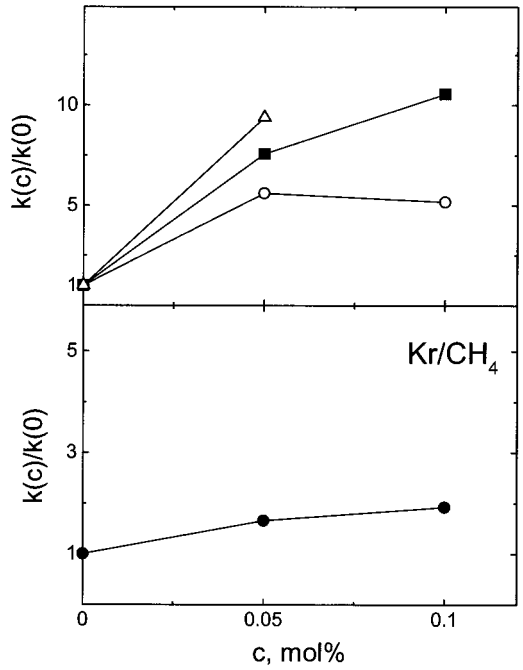

Figure 8. Dependence of the electron−ion recombination rate constant in Kr/CH_4 relative to its value in pure Kr on the concentration of CH_4. Comparison of the theoretical (lower part) and experimental[15] (upper part) results. The experimental results were determined at an external electric field of 450 V/cm (open circles), 600 V/cm (squares), and 750 V/cm (triangles).

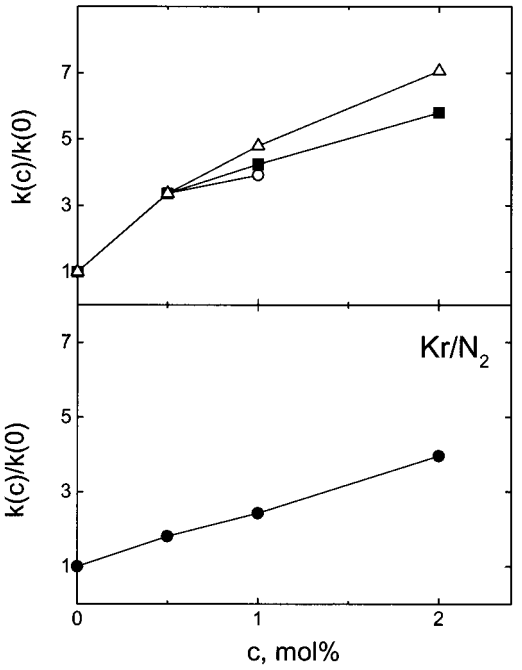

Figure 9. Dependence of the electron−ion recombination rate constant in Kr/N_2 relative to its value in pure Kr on the concentration of N_2. Comparison of the theoretical (lower part) and experimental[15] (upper part) results. The experimental results were determined at an external electric field of 450 V/cm (open circles), 600 V/cm (squares), and 750 V/cm (triangles).

to model the systems of a rather high density, we achieved a reasonable agreement with experiment in the calculations of the electron mobility.

For both Kr/CH_4 and Kr/N_2 systems we found that the electron−ion recombination rate constant increases with the concentration of the added molecular species. Such a behavior of k has been expected. Electrons in an ionized rare gas, due to their long mean free path, can be strongly accelerated by the Coulomb field of cations, and the acquired kinetic energy must be dissipated before the recombination is completed. In the presence of molecular additives, the interaction with their vibrational and rotational modes provides a much more efficient mechanism of dissipating electron energy compared with elastic collisions, which is the only available dissipation mechanism for a pure rare gas. While the rotationally inelastic collisions may significantly affect all stages of the recombination process, the collisional vibrational excitations, due to their high threshold energies, contribute mostly to the "final" stage of recombination, where electrons are localized in the vicinity of the cation and their average kinetic energy is high.

A comparison of the theoretical results for the recombination rate constant in Kr/CH_4 and Kr/N_2 systems with the experimental data of Takeda et al.[15] is presented in Figures 8 and 9, respectively.

The figures show the values of k relative to its value in pure Kr, as a function of the concentration of the molecular species. The experimental data were obtained in the presence of an external electric field, and the three data sets plotted in the upper parts of Figures 8 and 9 correspond to the field strengths of 450, 600, and 750 V/cm. The simulation results are shown in the lower parts of the figures. In the case of Kr/N_2 (Figure 9), a comparison of the experimental and the simulation data gives a reasonable agreement. The rate constant calculated for 2 mol % N_2 is 4 times higher than $k(c=0)$, which is comparable to the increase of 5.8 and 7 times observed experimentally at the external field of 600 and 750 V/cm, respectively. For Kr/CH_4 (Figure 8), the relative increase of k with c is slower in the theoretical results than in the experimental ones, and the simulation value for $k(c)/k(0)$ at $c = 0.1$ mol % is about 2, which is to be compared with the corresponding experimental values of 5 and 11, observed at the external field of 450 and 600 V/cm, respectively. When we compare the absolute values of the rate constant, the experimental results are significantly higher than the simulation ones. The simulation for pure Kr yields $k = 0.6 \times 10^{-7}$ cm^3/s, while the corresponding values of k reported by Takeda et al.[15] at the external field of 450, 600, and 750 V/cm are 3.5, 2.1, and 1.3×10^{-5} cm^3/s, respectively. The reasons for this disagreement have been thoroughly discussed in ref 14. One of the reasons might be the role of the external electric field applied in the experimental studies. The simulation results are calculated in the absence of an external field. In the earlier study by the group of Hatano[2] it was found that the recombination rate constant in Kr increases with the field strength in the region of low electric fields. The value of k measured at the lowest field of about 20 V/cm was 4.6×10^{-6} cm^3/s (cf. Figure 3 in ref 2), which is much closer to our simulation result than the values of Takeda et al.[15] cited above. By extrapolating the results of Hatano[2] to the zero field, we could reduce the discrepancy between the experiment and the theory even further. On the other hand, it is rather difficult to explain the observed increase of k with the field strength in the region of low fields. Since an external field increases the average kinetic energy of electrons, the recombination rate constant should rather decrease with increasing field,[11] as it is observed experimentally in the region of high fields. Another question is how the external electric field affects the recombination rate constant in the presence of molecular additives in Kr. The experimental data plotted in the upper parts of Figures 8 and 9 show that the effect of molecular additives on k becomes stronger as the electric field increases. This can be attributed to the enhanced dissipation of the electron energy in the rotational and vibrational collisions.

Admittedly, a detailed theoretical analysis of the effect of an external field on the electron−ion recombination in dense rare gases is still to be done.

The main question that motivated this study was whether the effects due to the presence of trace amounts of molecular impurities in experimental samples can account for the observed discrepancy between the theoretical and experimental results for the electron−ion recombination rate constant in dense rare gases. If this is true, the rate constant determined by simulation should increase much faster with increasing impurity concentration than it is observed in experiment. From Figures 8 and 9 we see that such a behavior of k has not been confirmed by our calculations. For the Kr/N_2 system, the increase of the calculated rate constant with c is comparable with experiment, and for Kr/CH_4 the increase of k with c is even slower in the simulation results. Therefore, we conclude that molecular species, which might have been present in trace amounts in measured gas samples, had no significant effect on the recombination rate constant. We need to find other reasons to explain the discrepancy between the theoretical and experimental results for k.

One possible reason, already discussed in ref 14, is the ion concentration effect on the recombination rate constant. At rather high densities of charges generated by X irradiation of gases in the experiments of the group of Hatano, the effects due to the superposition of the Coulomb field of neighboring cations may significantly affect the recombination process and make the recombination rate time-dependent. Another reason that needs to be considered is related to clustering of atoms in ionized rare gases. Rare gas cations are known to react with surrounding neutral atoms and form rare gas cluster cations. Rare gas cluster cations are rather large[28] and have a number of internal vibrational modes with rather high frequencies. Therefore, if an electron collides with a rare gas cluster ion, it will lose its kinetic energy quite efficiently, which should accelerate recombination. Further studies of those effects are needed in order to achieve a satisfactory agreement between theory and experiment.

Acknowledgment. We wish to thank Prof. Y. Hatano for helpful discussions and providing his experimental data prior to publication. This work was supported by the COE (Center of Excellence) development program of Science and Technology Agency of Japan. It was also supported in part (M.W.) by Grant No. 3 T09A 049 19 from the Polish State Committee for Scientific Research.

References and Notes

(1) Shinsaka, K.; Codama, M.; Srithanratana, T.; Yamamoto, M.; Hatano, Y. *J. Chem. Phys.* **1988**, *88*, 7529.
(2) Honda, K.; Endou, K.; Yamada, H.; Shinsaka, K.; Ukai, M.; Kouchi, N.; Hatano, Y. *J. Chem. Phys.* **1992**, *97*, 2386.
(3) Rice, S. A. *Diffusion-Limited Reactions*; Bamford, C. H., Tipper, C. F. H., Compton, R. G., Eds.; Comprehensive Chemical Kinetics 25; Elsevier: Amsterdam, 1985; p 47.
(4) Schmidt, W. F. *Liquid-State Electronics of Insulating Liquids*; CRC Press: Boca Raton, FL, 1997; p 121.
(5) Nakamura, Y.; Shinsaka, K.; Hatano, Y. *J. Chem. Phys.* **1983**, *78*, 5820.
(6) Shinsaka, K.; Codama, M.; Nakamura, Y.; Serizawa, K.; Hatano, Y. *Radiat. Phys. Chem.* **1989**, *34*, 519.
(7) Shinsaka, K.; Nakamura, Y.; Endou, K.; Honda, K.; Yamada, H.; Isoda, K.; Ukai, M.; Kouchi, N.; Hatano, Y. *Nucl. Instrum. Methods A* **1993**, *327*, 15.
(8) Warman, J. M. *J. Phys. Chem.* **1983**, *87*, 4353.
(9) Morgan, W. L. *J. Chem. Phys.* **1986**, *84*, 2298.
(10) Tachiya, M. *J. Chem. Phys.* **1987**, *87*, 4108.
(11) Wojcik, M.; Tachiya, M. *J. Chem. Phys.* **1998**, *109*, 3999.
(12) Sceats, M. G. *J. Chem. Phys.* **1989**, *90*, 2666.
(13) Kaneko, K.; Takimoto, J.; Usami, Y.; Kitahara, K. *J. Phys. Soc. Jpn.* **1990**, *59*, 56.
(14) Wojcik, M.; Tachiya, M. *J. Chem. Phys.* **1999**, *110*, 10016.
(15) Takeda, K.; Kato, R.; Hayashida, M.; Odaka, T.; Shinsaka, K.; Kameta, K.; Odagiri, T.; Kouchi, N.; Hatano, Y. *J. Chem. Phys.* **2001**, *114*, 3554.
(16) Hunter, S. R.; Carter, J. G.; Christophorou, L. G. *Phys. Rev. A* **1988**, *38*, 5539.
(17) Kowari, K.; Demeio, L.; Shizgal, B. *J. Chem. Phys.* **1992**, *97*, 2061.
(18) Krajcar-Bronic, I.; Kimura, M. *J. Chem. Phys.* **1995**, *103*, 7104.
(19) Skullerud, H. R. *J. Phys. D* **1968**, *1*, 1567.
(20) Rees, H. D. *J. Phys. Chem. Solids* **1969**, *30*, 643.
(21) Lin, S. L.; Bardsley, J. N. *J. Chem. Phys.* **1977**, *66*, 435.
(22) Northrup, S. H.; Allison, S. A.; McCammon, J. A. *J. Chem. Phys.* **1984**, *80*, 1517.
(23) Tachiya, M. *J. Chem. Phys.* **1988**, *89*, 6929.
(24) Itikawa, Y.; Hayashi, M.; Ichimura, A.; Onda, K.; Sakimoto, K.; Takayanagi, K.; Nakamura, M.; Nishimura, H.; Takayanagi, T. *J. Phys. Chem. Ref. Data* **1986**, *15*, 985.
(25) Phelps, A. V. Available at ftp://jila.colorado.edu/collision_data/electron.txt.
(26) Onda, K. *J. Phys. Soc. Jpn.* **1985**, *54*, 4544.
(27) Gerjuoy, E.; Stein, S. *Phys. Rev.* **1955**, *97*, 1671.
(28) Itoh, K.; Holroyd, R. A.; Nishikawa, M. *J. Phys. Chem. A* **2001**, *105*, 703.